Photosynthesis Research **31**: 213–226, 1992.

Regular paper

Theory of the optical spectra of the bacteriochlorophyll *a* antenna protein trimer from *Prosthecochloris aestuarii*

Robert M. Pearlstein
Physics Department, Indiana-Purdue University, Indianapolis, IN 46205, USA

Received 5 August 1991; accepted in revised form 4 November 1991

Key words: circular dichroism, exciton states, laser hole-burning, photosynthetic bacteria, protein structure

Abstract

A reasonable theoretical fit to the experimental low-temperature absorption and CD spectra of the BChl *a*-protein from *Prosthecochloris aestuarii* has been obtained for the unaggregated protein trimer based on standard assumptions regarding Q_Y transition moment directions. The fits depend to some extent upon varying the site wavelengths of the individual BChls not just in one subunit but in the entire trimer, a procedure not tried before. Features in both spectra, but especially in CD, at wavelengths longer than ≈810 nm are very strongly influenced by the intersubunit interactions of BChls 7 (in the Fenna-Matthews numbering). Unlike earlier theoretical models, which also gave reasonable fits but were based on unorthodox or incorrect assumptions, this exciton model gives every indication of being refineable by improved choices of site wavelengths and exciton-transition lineshapes. Calculated exciton-transition wavelengths and line widths are compared with values deduced from recent laser hole-burning experiments (Johnson and Small 1991). As in the case of the absorption and CD spectra, agreement is best for the long-wavelength half of the Q_Y region.

Abbreviations: CD – circular dichroism; BChl – bacteriochlorophyll

1. Introduction

Interpretation of the optical spectra of the BChl *a*-protein from *Prosthecochloris aestuarii* is a longstanding problem that has resisted a number of attempts at solution. This has been both puzzling and frustrating. It is puzzling because an enormous amount is known, both experimentally and theoretically, regarding this protein. This knowledge includes the three-dimensional structure of the protein at near-atomic resolution (Fenna and Matthews 1975, Fenna et al. 1977, Matthews et al. 1979, Tronrud et al. 1986), exceptionally well-resolved low-temperature optical spectra (Philipson and Sauer 1972, Whitten et al. 1978a), almost unambiguous theoretical description of the BChl molecular Q-orbitals (Weiss 1972, Hanson 1988), and the straightforward physics of the (exciton) interactions of transition dipoles (Pearlstein 1991). It is frustrating because of initial high hopes that the protein might serve as a 'Rosetta stone' for the interpretation of antenna protein spectra. These hopes arise because BChl interactions in the *P. aestuarii* protein are particularly simple: unlike BChls in reaction centers, and presumably unlike those in intramembrane antenna complexes, in the *P. aestuarii* protein there are no BChl van der Waals dimers to complicate spectral interpretations.

As has been reviewed several times (Pearlstein 1982, 1987, 1991), with one exception early at-

tempts to simulate the spectra theoretically gave poor agreement with experiment. The exception (Pearlstein and Hemenger 1978) required an unorthodox molecular orbital assumption that has never been justified; this simulation is now viewed simply as a coincidental result. A more recent theoretical study (Pearlstein 1988) was based on the assumption that, under the conditions of the low temperature optical spectroscopy, the *P. aestuarii* protein (itself a trimer of identical subunits) aggregates to produce new inter-β-sheet contacts creating additional strong exciton interactions between BChls not in the same trimer. New computer graphics results, presented here, demonstrate that even if such β-sheet contacts exist they can at most lead to intertrimer exciton interactions that are too weak to have any significant effect on the spectra.

Although the hypothetical inter-β-sheet aggregates, which could not be large under the experimental conditions for spectroscopy, thus fail to explain the optical spectra, a computer study (Pearlstein, unpublished) in which such an aggregate forms a large ring of the protein trimers inspired the present work. That study provides an example of the general principle (Pearlstein and Zuber 1985) that a set of exciton interactions related by a rotational symmetry can produce spectral effects larger than expected on the basis of one of them alone. The isolated protein trimer, which is usually thought to be the object of spectroscopic study, itself exhibits such a rotational symmetry, namely C-3. At least two previous theoretical efforts (Pearlstein and Hemenger 1978, Meister 1986) included comparative calculations of protein trimer and protein subunit spectra. No significant differences were found – see section 3.4. For this reason, although no intact, isolated protein subunit has ever been observed experimentally, the simpler protein subunit has been favored for theoretical work. However, the earlier calculations of trimer spectra overlooked an aspect of BChl interactions that has been considered in subunit spectral calculations, i.e., variation of 'site wavelengths'. Because each of the 7 inequivalent BChls in a subunit may have a distinct set of interactions with protein moieties, even were there no exciton interactions the 7 BChls may absorb at different ('site') wavelengths in the Q_Y region. Even when the 7 site wavelengths are treated as independently adjustable parameters, no reasonable simultaneous fit to absorption and CD spectra could be found from subunit calculations. It was (erroneously) assumed that since subunit and trimer calculations give similar results for a common site wavelength, they also do so with distinct site wavelengths. In order to fully explore the consequences of the trimer's C-3 symmetry on the exciton interactions, and hence on the simulated spectra, it is necessary to avoid this assumption. This forms the basis of the present work.

Calculated absorption and CD spectra are presented and compared with the experimental spectra in section 3. In addition, the site wavelengths chosen for these calculations are compared with the site-wavelength ranges calculated for each of the 7 BChls on the basis of molecular orbital theory by Gudowska-Nowak et al. (1990). The exciton-transition wavelengths calculated here, and the chosen values of the (Gaussian) transition line widths, are compared with the corresponding numbers deduced by Johnson and Small (1991) from their laser hole-burning spectra of the *P. aestuarii* protein.

2. Theoretical methods

Calculations of exciton stick spectra and Gaussian synthesis of simulated absorption and CD spectra are performed by standard methods (Pearlstein 1991). In these calculations, the Q_Y transition of each of the 21 BChl molecules in the protein trimer is included, as are the interactions of all pairs of these transitions. The Q_X and higher transitions are neglected. The pairwise Q_Y–Q_Y interactions are calculated in the point monopole approximation with the distribution of transition charges obtained by Weiss (1972). Here, the Weiss charges are scaled by a factor of 1.1686, which is the ratio of the Q_Y transition dipole moment used here to that calculated by taking the sum of the product of each original Weiss charge with its vector distance from the molecular center projected along the BChl Y-axis. The value of the Q_Y transition dipole moment used here, $51.6\,D^2$, corresponding to the round value of 260 in formula units ($5.04\,\mu^2$),

roughly equals the value ($52\,D^2$) used by Pearlstein and Hemenger (1978), which itself was based on Fenna's value (Fenna RE, personal communication) of $50.8\,D^2$. Strictly speaking, one ought not to scale the Weiss monopoles in this way, because insofar as the increased Q_Y dipole strength is 'borrowed' from higher transitions the mix of the elementary Y-orbital transitions ($a_{1u} \rightarrow e_{gx}$ and $a_{2u} \rightarrow e_{gy}$, which make up the Q_Y in the 4-orbital scheme) is changed. However, this is clearly a higher order correction for BChls far enough apart that the transition monopole method itself gives a relatively small correction over the point transition dipole method, as is the case here.

Computer graphics investigation of details of the protein structure are performed on a Silicon Graphics SGI 220 computer with the aid of the Polygen 'Quanta' software. Atomic coordinates of the BChl *a*-protein are obtained from the Brookhaven Protein Data Bank, as supplied by Tronrud et al. (1986).

3. Results and discussion

3.1. Intersubunit interactions

Two types of intersubunit exciton interactions between BChls may be distinguished, those that occur between subunits belonging to the same trimer, and those that arise from interacting subunits belonging to different trimers. In a previous paper (Pearlstein 1988), it is noted that some of the exciton interactions of the second type may become quite large, comparable in magnitude to the nearest-neighbor intrasubunit interactions, if the flat β-sheet sections of two subunits are placed in van der Waals contact. The assumption of that paper, that such a juxtaposition of subunits is possible at least in principle, is based on the published description of the β-sheet structure (Matthews et al. 1979). However, examination of the β-sheet on the graphics computer shows that this description, while certainly correct, is incomplete. The published description asserts, and the graphics computer confirms, that the α-carbons of residues 7–13, 21–27, 259–265, 243–250, 42–48, 60–66 and 73–79 (ranges lying in consecutive strands) lie very nearly in a single plane, with the α-carbons of residues 7, 13, 73 and 79 defining the extremes of this planar region, which is very nearly a rectangle. It has not previously been noted that this α-carbon plane lies on the *inside* of the protein. The progression of the polypeptide backbone, and the residues themselves, project outward from the flat α-carbon plane, forming a highly corrugated protein surface in that region. Using the interatomic distance calculator built in to the 'Quanta' software, one finds that the protein surface is ~6 Å from the (internal) α-carbon plane. Thus, the minimum center-center separation of the BChls 5 in two subunits juxtaposed at their 'flat' β-sheets is ~12 Å more than that calculated previously, i.e., a total separation >25 Å. The result is that the large intersubunit exciton interaction calculated previously ($178\,cm^{-1}$) must be reduced by an order of magnitude. The interaction is then too small, by itself, to significantly affect details of the optical spectra. (See the discussion at the end of section 3.)

The minimum nearest-neighbor separation of BChls lying in different subunits of the same trimer is ~24 Å, and therefore one expects the corresponding exciton energies to be comparably small. Because the C-3 symmetry of the trimer may 'amplify' them, especially in CD spectra, the effects of these smaller energies need to be re-examined. Table 1 shows all of the distinct BChl Q_Y–Q_Y interaction energies calculated in the point monopole approximation. Within each subunit, where the center-center separations of nearest-neighboring BChls are ~12 Å, the largest energies are in the range of ~50–200 cm^{-1}, occurring between BChl pairs 1–2, 2–3, 3–4, 4–5, 4–7, 5–6 and 6–7. In contrast, the largest intersubunit energies are ~20 cm^{-1}. The single largest intersubunit interaction, 20.8 cm^{-1}, occurs between a BChl 2 of one subunit and a BChl 5 of another. However, since only two subunits are coupled by each of these 20.8-cm^{-1} interactions, they do not introduce effects of the trimer's C-3 symmetry. The second-largest intertrimer interaction, 16.3 cm^{-1}, coupling all three pairs of BChls 7, does introduce C-3 symmetry effects. It is noteworthy that the next largest C-3-symmetric intertrimer interaction, that of magnitude 5.3 cm^{-1} coupling all three pairs of

Table 1. Energies of trimer BChl Q_Y–Q_Y interactions in the point monopole approximation[a]

1 **9** **17**	**2** **10** **18**	**3** **11** **19**	**4** **12** **20**	**5** **13** **21**	**6** **14**	**7** **15**	**8** **16**	
(*801.9*)								
12.4700	−0.1879	0.0101	−0.0092	0.0113	−0.0237	−0.0091	0.0028	**1**
0.0038	0.0035	0.0005	0.0018	0.0000	0.0012	0.0028	0.0009	
−0.0014	−0.0003	0.0070	0.0038	0.0021				
	(*801.9*)							
	12.4700	0.0516	0.0130	0.0026	0.0192	0.0061	0.0009	**2**
−0.0011	0.0005	0.0006	0.0024	0.0017	0.0006	0.0038	−0.0011	
−0.0057	−0.0102	***0.0208***	0.0122	0.0033				
		(*800.0*)						
		12.5000	−0.1014	−0.0017	−0.0161	0.0137	−0.0014	**3**
−0.0058	−0.0048	0.0002	0.0031	0.0015	−0.0018	0.0035	0.0005	
−0.0048	0.0075	0.0122	0.0044	0.0108				
			(*787.4*)					
			12.7000	−0.1326	−0.0277	−0.0977	−0.0003	**4**
−0.0102	0.0075	0.0053	−0.0013	0.0042	0.0109	0.0005	0.0006	
0.0002	0.0053	−0.0023	−0.0006	0.0050				
				(*800.0*)				
				12.5000	0.1036	0.0007	0.0070	**5**
0.0208	0.0122	−0.0023	0.0047	−0.0044	−0.0029	0.0018	0.0024	
0.0031	−0.0013	0.0047	−0.0004	−0.0015				
					(*813.0*)			
					12.3000	0.0713	0.0038	**6**
0.0122	0.0044	−0.0006	−0.0004	−0.0037	0.0011	0.0000	0.0017	
0.0015	0.0042	−0.0044	−0.0037	0.0053				
						(*822.0*)		
						12.1650	0.0021	**7**
0.0033	0.0108	0.0050	−0.0015	0.0053	***0.0163***	0.0012	0.0006	
−0.0018	0.0109	−0.0029	0.0011	***0.0163***				

[a] Units are thousands of cm^{-1}, except for italicized numbers in parentheses, which are the wavelengths in nm corresponding to the BChl site energies (underlined). Bold face numbers at the top and right margins designate the BChl molecules in the numbering scheme of Fenna and Matthews (1975). The largest intersubunit interactions are shown in bold-face italics. Interaction energies for BChl pairs not listed may be found by taking advantage of pair and C-3 symmetries; for example, E (18, 6) = E (6, 18) and E (8, 21) = E (1, 14).

BChls 4, is more than a factor of three smaller. Clearly, the relatively large C-3-symmetric couplings of the BChls 7 merit closer attention.

3.2. Sequentially determined site wavelengths

Provided the BChl site wavelengths are all the same, any effects of intersubunit exciton couplings on optical spectra are generally masked by the effects of the much larger interactions between nearest neighbors inside each subunit. However, if a particular BChl has a highly shifted site wavelength relative to the others, spectral effects of its strong exciton interactions diminish (Pearlstein 1982). On the other hand, since the three subunits are all identical, a particular BChl in one subunit must have the same site wavelength as the corresponding BChl in each of the other two subunits. Thus, if one assumes that BChl 7 has a substantial differential site wavelength relative to the other six BChls in the subunit (especially 4 and 6), one can expect

the spectra to manifest effects of the C-3-symmetric couplings of the BChls 7. Here, this is the starting assumption in choosing a set of site wavelengths. The differential site shift of the BChls 7 must be to longer wavelengths if one is to explain effects at the long-wavelength edge of the Q_Y absorption and CD bands (see below).

Earlier studies (Pearlstein and Hemenger 1978, Pearlstein 1988) have shown that, if all BChls have a common site wavelength, the highest absorption peak in the low temperature absorption spectrum is best fit if that wavelength is 802.6 nm. Thus, the first step in sequentially choosing a set of site wavelengths to fit the experimental spectra is to set the site wavelength of the BChls 7 at a value significantly larger than 802.6 nm, indeed at a value close to that of the longest wavelength peak (~825 nm) in the absorption spectrum. Note that this peak has an integrated extinction corresponding to ~1 BChl/subunit, which is consistent with the assumption that the BChls whose absorption gives rise to it are relatively well site-shifted from the other BChls.

Discussion of the sequential choice of other site wavelengths is facilitated by reference to Table 2, which provides a guide to the effects of the largest exciton pair-interactions. A given pair can be expected to influence the absorption spectrum, at least qualitatively, according to the tabulated 'shift tendency', unless the members of that pair have well separated site wavelengths. Of course, quantitative determination of the spectral effects of a given choice of site wavelengths requires a full calculation of the spectra for that choice. The arguments presented here merely help to reduce the number of full calculations required. In Table 2, the splitting energy is twice the Q_Y–Q_Y interaction listed in Table 1. The shift tendency indicates the direction (red = 'toward longer wavelengths', blue = 'toward shorter wavelengths') in which squared transition dipole strength would be shifted if the BChl pair were an isolated exciton dimer. The last column gives the fraction of the total transition strength (of the two BChls) that would reside in the stronger of the two exciton components, for the pair as an isolated dimer with each of the two BChls having the same site wavelength.

Having begun by tentatively choosing the BChl 7 site wavelength, one observes from Table 2 that BChls 4 and 6 have the strongest interactions with 7. Thus, the choice of site wavelengths for 4 and 6 must have a large influence on the absorption near 825 nm, otherwise dominated by 7. Clearly, since the 4–7 interaction produces an overwhelming red shift, one reasons that the effect of this interaction should be reduced as much as possible, otherwise the absorption becomes much too great at long wavelength. By this reasoning, the site wavelength of BChl 4 should be much shorter than that of BChl 7. Logically, then, the 6–7 interaction must dominate spectral effects in the ~815–825 nm region. The site wavelength of BChl 6 is thus chosen to lie closest to that of BChl 7, but not so close as to pull too much strength from the 825-nm peak.

Besides 7, BChl 5 is the only other that interacts strongly with 6. According to Table 2, the 5–6 interaction is a moderate red shifter. Thus, BChl 5's site wavelength must be placed well to the blue of 6's in order to gain substantial strength in the 815-nm region, where the absorption is maximal, and to avoid too much interference with the effects of the 6–7 interaction on the 815–825 nm region. It is difficult to extend the foregoing arguments to the placement of site wavelengths for BChls 1–3, other than to note

Table 2. Exciton-pair shift tendencies

BChl pair	Splitting energy (cm^{-1})	Shift tendency	Fraction of total squared dipole strength in major component
1 & 2	376	red	0.71
2 & 3	103	blue	0.85
3 & 4	203	blue	0.54
4 & 5	265	red	0.59
4 & 7	195	red	0.94
5 & 6	207	red	0.72
6 & 7	143	blue	0.68

that they must all lie to the blue of 6's, again to avoid interference with the effects of the 6–7 interaction.

In practice, this sequential fitting of the site wavelengths proceeds by choosing tentative values based on the foregoing for BChls 5–7 and keeping those of 1–4 well to the blue. The site values for 5–7 are then somewhat refined in a series of calculations concerned only with fitting the red halves of the absorption and CD spectra to experiment. Finally, with site wavelengths for 6 and 7 more-or-less fixed, the other site wavelengths are varied to produce the best fitting spectra overall. (To reduce the number of search parameters, site wavelengths of 1 and 2, and of 3 and 5, are set equal. Since the 1–2 interaction is a moderate red shifter with a big splitting energy, equating the site wavelengths of these two helps to keep the total absorption band within reasonable bounds; i.e., though their site wavelengths lie somewhat to the blue, a large fraction of their strength is shifted back toward the band center.) Here, 'best fitting' means simply as judged by eye.

As noted in the Introduction, the site wavelengths have to be treated as fitting parameters because there is, at present, no experimental method for determining them in situ. However, a theoretical study of these wavelengths for the BChls of the *P. aestuarii* protein, based on detailed molecular orbital calculations, has been performed by Gudowska-Nowak et al. (1990). Unfortunately, present uncertainties in the number and degree of ionization of charged amino acid residues in the vicinity of each of the BChls limits the usefulness of their findings, summarized in Fig. 1. As can be seen, for most of the BChls the ranges determined by Gudowska-Nowak et al. are extremely broad. It is therefore of only slight interest that the site wavelengths determined in this work fit well inside those broad ranges for BChls 4–7. More interesting is the disagreement for the other BChls. In particular, this work's site wavelengths lie well outside the ranges calculated by Gudowska-Nowak et al. for BChls 1 and 3. While great precision certainly cannot be claimed for the current fitted values of the 1 and 3 site wavelengths, it is clear on experimental grounds that the entire ranges of Gudowska-Nowak et al. simply lie too far to the blue (in the case of BChl 3, much too far) for those BChls. Since the ranges encompass most sources of uncertainty, and there is substantial evidence the molecular orbital calculation used (INDO/s) is quite reliable, one must look to what is left out of the calculation for the source of the 'missing' red shift. A good possibility, and one noted by Gudowska-Nowak et al., is a mechanism based on collective, long-range electrostatic effects inside the protein. Currently, this is very difficult to calculate, and thus it is unlikely that reliable site-wavelength values will be calculated soon. Indeed, it is more likely that precise values will be obtained first from improved fitting methods (see below).

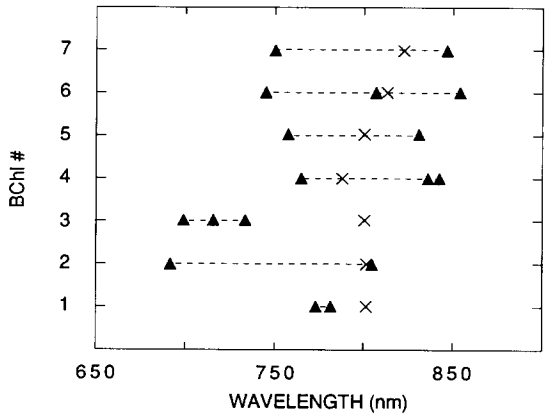

Fig. 1. Delimiting site-wavelength ranges of the 7 inequivalent BChls, based on the calculations of Gudowska-Nowak et al. (1990). For each BChl, the solid triangles indicate the calculated values, corresponding to 0, 1, or more fully charged amino acid residues. The dashed lines are drawn on the assumption that partially charged residues produce intermediate site-wavelength values. However, one can infer that the ranges for BChls 3, 4 and 6 may extend to somewhat longer wavelengths than indicated (still leaving the range for BChl 3 too narrow to encompass the current fit point); see Table 6 of Gudowska-Nowak et al. The symbol '×' denotes the best-fit value of the present work.

3.3. *'Best' fits*

Results for the current best-fit site wavelengths are given in Tables 3 and 4, and Fig. 2. Table 3 lists the calculated spectral parameters for the 21 Q_Y exciton transitions, 7 of which are nondegenerate and 14 of which occur in degenerate pairs as a result of the C-3 symmetry. Table 4, which gives the eigenvectors for the 21 transi-

Table 3. Trimer Q_Y exciton stick-spectra for 'best-fit' site wavelengths[a]

Exciton transition[b] #	Energy ($k\,cm^{-1}$)	Wavelength (nm)	Dipole strength[c] (D^2)	Rotational strength[c] (DBM)	Absorption width[d] (cm^{-1})	CD width[d] (cm^{-1})
1	12.825	779.7	75.8	25.3	170	160
2, 3	12.814	780.4	12.9	−14.0	170	160
4, 5	12.668	789.4	30.6	−20.2	170	160
6	12.662	789.8	20.1	26.3	170	160
7, 8	12.541	797.4	25.8	2.6	170	160
9	12.507	799.6	24.7	43.4	170	160
10	12.442	803.8	38.1	−9.2	170	160
11, 12	12.414	805.5	112.9	−13.8	80	160
13	12.300	813.0	117.6	84.8	85	120
14, 15	12.281	814.3	90.3	6.2	85	120
16	12.274	814.7	102.2	−65.5	85	120
17, 18	12.265	815.3	25.7	−8.8	85	120
19	12.134	824.1	93.1	−37.5	80	120
20, 21	12.101	826.4	7.7	14.2	80	200

[a] From Table 1.
[b] Two transitions listed on one line are degenerate.
[c] For degenerate pairs, strength is listed per transition.
[d] Widths are assigned *ad hoc*. See text.

Table 4a. Exciton eigenvectors for non-degenerate transitions[a]

Transition #	Amplitude[b,c] on BChl:						
	1 8 15	2 9 16	3 10 17	4 11 18	5 12 19	6 13 20	7 14 21
1	−0.005	−0.040	−0.155	0.486	−0.243	−0.078	−0.078
6	−0.402	0.403	0.048	0.058	0.005	0.057	0.016
9	0.008	0.006	0.381	−0.097	−0.383	−0.179	0.013
10	−0.163	−0.064	−0.381	−0.273	−0.273	−0.086	0.034
13	0.046	−0.035	0.022	0.034	−0.183	0.443	0.314
16	0.378	0.405	−0.126	−0.049	−0.083	−0.035	0.006
19	−0.011	0.002	−0.023	0.078	0.112	−0.295	0.476

[a] From Table 3.
[b] The squared amplitude is the probability for that BChl to be excited in the indicated transition.
[c] These have C-3 symmetry.

tions, shows that, in each case, only one or two of the BChls (per subunit) contributes much of the squared amplitude; i.e., with these site wavelengths none of the exciton states is highly delocalized within a subunit. As a result, the extreme transition wavelengths of the exciton band, 780 and 826 nm from Table 3, differ little from the extreme site wavelengths, 787 and 822 nm from Table 1. Also, because of the relatively limited exciton delocalization, one expects not very much exciton narrowing of absorption and CD spectra (Pearlstein 1982). For this reason, and also because questions have been raised (Small GJ, personal communication) about the validity of theoretical models that predict such narrowing effects, Gaussian widths have been assigned individually to the exciton transitions, as indicated in Table 3. The tabulated widths are the full widths at half maximum of the symmetric Gaussians, one per transition (two identical ones per degenerate transition pair), chosen to within $\pm 5\,cm^{-1}$ to give the best fit by eye. It is encouraging that essentially only two different widths are needed for each spec-

Table 4b. Exciton eigenvectors for degenerate transitions[a]

Transition #	Amplitude[b] on BChl:						
	1 8 15	2 9 16	3 10 17	4 11 18	5 12 19	6 13 20	7 14 21
2	0.036 −0.014 −0.021	−0.045 0.042 0.002	0.164 0.047 −0.210	−0.530 −0.123 0.653	0.252 0.047 −0.299	0.093 0.011 −0.104	0.103 0.012 −0.115
3	0.004 −0.033 0.029	0.023 0.027 −0.050	0.148 −0.216 0.068	−0.448 0.683 −0.235	0.199 −0.318 0.118	0.066 −0.114 0.048	0.073 −0.126 0.052
4	−0.301 0.546 −0.246	0.312 −0.577 0.265	0.120 −0.156 0.036	−0.040 −0.009 0.049	−0.033 0.035 −0.003	0.014 −0.044 0.030	0.017 −0.024 0.007
5	0.457 0.032 −0.489	−0.486 −0.027 0.514	−0.111 −0.048 0.159	−0.033 0.051 −0.018	0.022 0.017 −0.039	−0.043 0.009 0.034	−0.018 −0.006 0.023
7	0.008 −0.157 0.149	−0.005 0.012 −0.006	0.232 −0.556 0.324	−0.074 0.089 −0.015	−0.250 0.487 −0.237	−0.128 0.275 −0.148	−0.011 0.020 −0.009
8	0.177 −0.081 −0.095	−0.010 0.001 0.010	0.508 −0.053 −0.455	−0.060 −0.034 0.094	−0.419 −0.007 0.426	−0.244 0.012 0.233	−0.017 −0.001 0.018
11	−0.087 −0.084 0.171	−0.027 −0.023 0.050	−0.288 −0.200 0.488	−0.184 −0.197 0.381	−0.191 −0.268 0.459	−0.068 −0.094 0.162	0.032 0.064 −0.096
12	−0.147 0.149 −0.002	−0.043 0.045 −0.002	−0.397 0.448 −0.051	−0.334 0.326 0.007	−0.420 0.375 0.044	−0.147 0.133 0.015	0.092 −0.074 −0.018
14	0.089 0.050 −0.139	0.129 0.115 −0.243	−0.063 −0.065 0.128	−0.028 −0.041 0.068	0.070 0.203 −0.273	−0.222 −0.407 0.630	−0.115 −0.163 0.278
15	−0.110 0.131 −0.023	−0.207 0.215 −0.009	0.112 −0.111 −0.001	0.063 −0.055 −0.008	−0.275 0.198 0.077	0.599 −0.492 −0.107	0.255 −0.227 −0.028
17	−0.467 0.009 0.459	−0.459 0.022 0.437	0.118 0.015 −0.132	0.034 0.000 −0.034	0.113 −0.005 −0.108	−0.166 −0.067 0.232	−0.093 −0.030 0.123
18	0.260 −0.534 0.275	0.240 −0.518 0.278	−0.085 0.144 −0.060	−0.020 0.039 −0.019	−0.060 0.128 −0.068	0.173 −0.230 0.057	0.088 −0.125 0.036
20	0.001 −0.003 0.001	0.007 −0.006 −0.002	−0.024 0.022 0.002	−0.110 −0.028 0.139	−0.088 −0.028 0.116	0.206 0.074 −0.280	−0.558 −0.140 0.698
21	−0.002 0.000 0.002	−0.003 −0.005 0.008	0.011 0.015 −0.027	−0.096 0.144 −0.048	−0.083 0.118 −0.035	0.204 −0.281 0.077	−0.484 0.725 −0.242

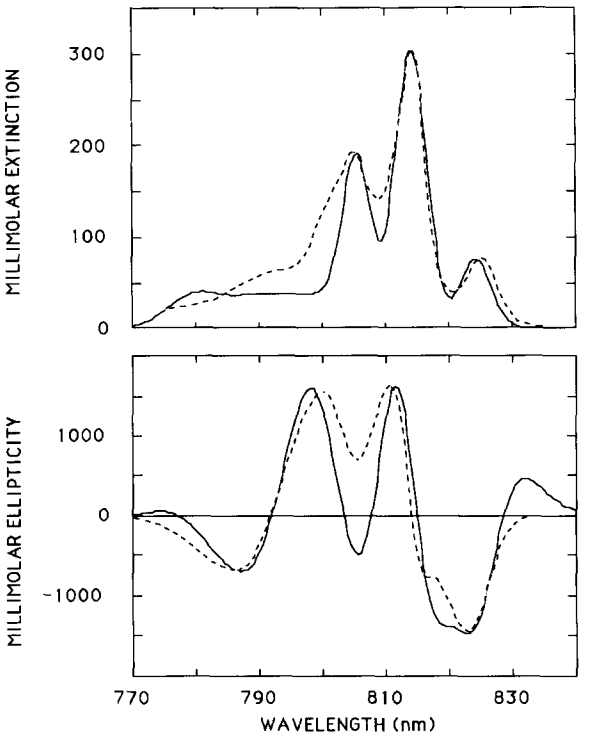

Fig. 2. Theoretical spectra (solid curves) computed from the Gaussian components listed in Table 3. Dashed curves are experimental absorption (Whitten et al. 1978) and CD (Philipson and Sauer 1972) spectra shown for comparison.

trum, absorption and CD, to achieve this fit. (The distinction between the 80- and the 85-cm^{-1} widths in absorption is not deemed 'essentially' different; the 200-cm^{-1} width assigned to transitions 20 and 21 in CD is completely arbitrary.) That the widths of absorption components should be less than those of CD components, as is the case here for transitions 11–19, is plausible because of the additional spectral narrowing experimentally observed on lowering the temperature from 77 K (at which the CD spectrum was obtained) to 5 K (at which the absorption spectrum was obtained). It is unclear why components of the short wavelength half of either spectrum are so much broader than those of the long wavelength half, nor why those widths are virtually the same for the two different spectra. One may speculate that this is due to a combination of factors, including misassignment of some site wavelengths and an unsophisticated method for determining spectral line shapes; see section 3.5.

Perhaps the most striking feature of Fig. 2 is how well the calculated CD spectrum agrees with experiment. Indeed, there are only two significant points of disagreement, the overly deep trough at 805.5 nm (though at precisely the right wavelength) and the spurious peak at 832 nm. On the other hand, the calculated absorption spectrum, while fitting rather well at wavelengths longer than ~805 nm, fits poorly at shorter wavelengths. This situation contrasts with the results of earlier model calculations. However, this may have no particular significance; it may be possible to find site wavelengths that improve both spectra simultaneously.

A general problem with the absorption fit is that the area under the calculated spectrum is ~15% less than that of the experimental spectrum. This means that the Q_Y dipole strength per BChl used here (see Theoretical methods), 51.6 D^2, may have to be increased in any future calculation to ~60 D^2 to obtain a precise overall fit. Actually, the higher strength accords more closely with the best measured value of the peak molar extinction of the BChl Q_Y band in the *P. aestuarii* protein, i.e., 154 000, on the basis of which a Q_Y dipole strength of 68.9 D^2 was calculated (Olson 1966). It remains to be explained why this strength is ≈50% larger for BChl in the complex as compared to BChl in a solvent.

3.4. Comparative results for subunit and trimer

The significance of the current best-fit spectra may be better understood in a comparative context. Such a context is provided by the calculated spectra shown in Figs. 3–5. In each case, the off-diagonal elements of the exciton interaction matrix are as in Table 1 (or a fraction of it for a calculation involving only one subunit); the stick spectra are not shown. As in the case of the 'best-fit' site wavelengths, the Gaussian component widths are chosen for greatest resemblance, by eye, to the experimental spectra. Results for a trimer whose BChls have the common site wavelength giving the best fit to absorption appear in Fig. 3. One sees that, in contrast to the best-fit theory, the 825-nm absorption peak is entirely missing in this simulation. The theoretical CD spectrum has only positive strength for $\lambda \geq$ ~820 nm, and has a strong trough at 810 nm

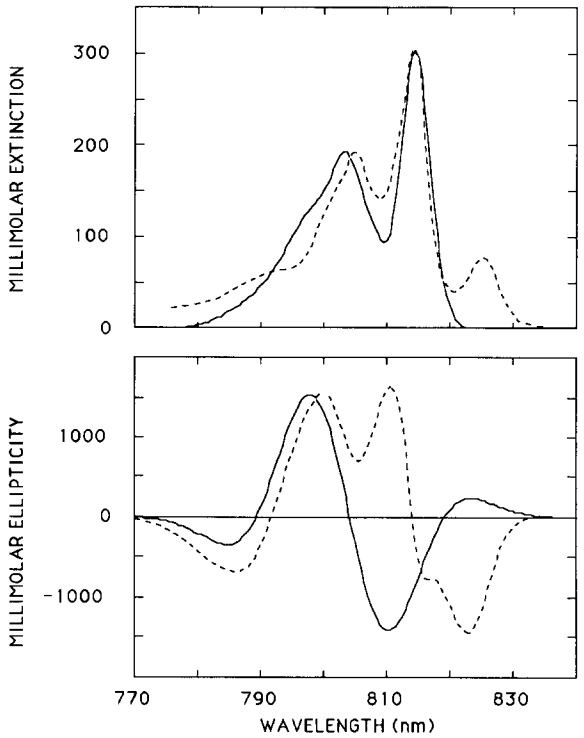

Fig. 3. Theoretical spectra (solid curves) for a trimer with a common site wavelength of 802.6 nm. The absorption spectrum is synthesized from symmetric Gaussians having full-widths at half maximum of 170 cm^{-1} each for exciton transitions 1–10, 80 cm^{-1} for transitions 11–15, and 70 cm^{-1} for transitions 16–21. For CD, each of the 21 symmetric Gaussians has width 240 cm^{-1}. As in Fig. 2, experimental spectra are shown for comparison (dashed curves).

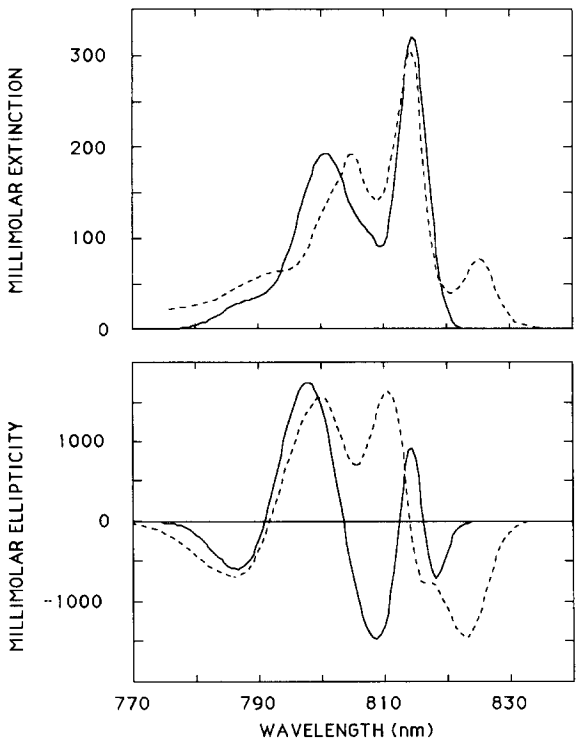

Fig. 4. Theoretical spectra (solid curves) for a subunit with a common site wavelength of 802.6 nm. For absorption, Gaussian widths are 170 cm^{-1} for exciton transitions 1 and 2, 130 cm^{-1} for transitions 3 and 4, 70 cm^{-1} for transition 5, and 80 cm^{-1} for transitions 6 and 7. For CD, widths are 170 cm^{-1} for transitions 1–5, and 70 cm^{-1} for transitions 6 and7. Dashed curves are experimental spectra (see Fig. 2).

where the experimental spectrum has a strong peak. Figure 4 shows theoretical absorption and CD for a single subunit with the same common site wavelength as in Fig. 3. It may be seen that the simulated absorptions of Figs. 3 and 4 are quite similar, as has been noted before, with the trimer absorption (Fig. 3) a marginally better fit at short wavelength. The simulated CDs are also similar; although a little different in detail, both give poor fits to experiment. The general similarity of the calculated spectra shown in Figs. 3 and 4 is, as already noted, the reason calculations using the entire trimer have seldom been done.

Calculated spectra for a single subunit having the best-fit site wavelengths are shown in Fig. 5. Although the subunit and trimer (Fig. 2) absorption spectra are nearly the same, the two CD spectra differ quite a bit. Indeed, the integral of the absolute value of the difference between experimental and theoretical ellipticities (a measure of goodness-of-fit) is smaller by more than a factor of two in Fig. 2 as compared to Fig. 5. The calculated trimer CD (Fig. 2) fits noticeably better at almost all wavelengths, and especially in the region around 820 nm. The only exception is in the vicinity of 830 nm, where the calculated trimer spectrum exhibits a spurious peak.

Taken together, Figs. 2–5 show that use of the whole trimer in calculations, rather than just one subunit, adds relatively little to the goodness-of-fit of theoretical absorption spectra, at least for the choices of site wavelengths made here. However, the trimer appears to play an important role in the formation of the long wavelength CD band. Thus, the relatively small intersubunit interactions of BChls 7, with their C-3 symmetry,

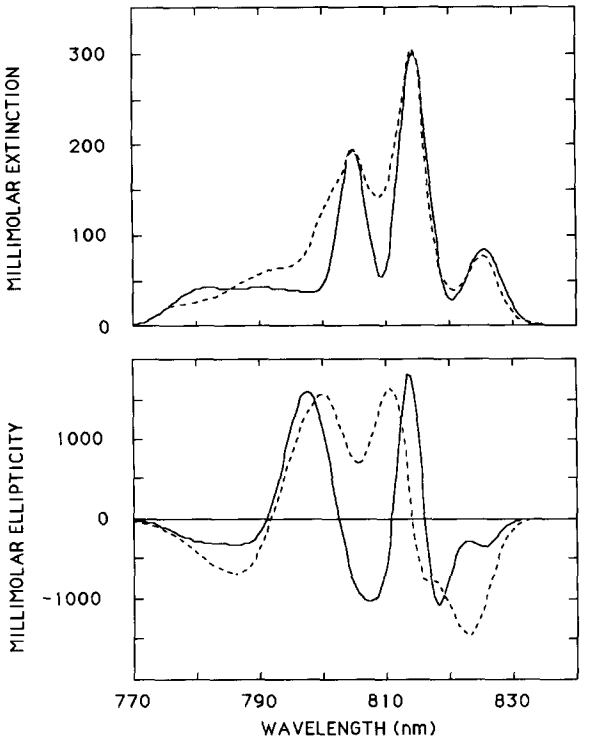

Fig. 5. Theoretical spectra (solid curves) for one subunit of the trimer whose site wavelengths are as in Fig. 2. For absorption, Gaussian widths are 170 cm^{-1} for exciton transitions 1–3, 80 cm^{-1} for transitions 4–6, and 100 cm^{-1} for transition 7. For CD, widths are 160 cm^{-1} for transitions 1, 2, and 4, 140 cm^{-1} for transition 3, 75 cm^{-1} for transitions 5 and 7, and 110 cm^{-1} for transition 6. Dashed curves are experimental spectra (see Fig. 2).

are quite significant in determining the strong double-trough feature of that band.

3.5. Comparison with results of laser hole-burning spectroscopy

Using the technique of persistent non-photochemical hole-burning, Johnson and Small (1991) have experimentally determined the transition energies and wavelengths of 8 of the 14 distinct BChl Q_Y exciton transitions in the *P. aestuarii* protein trimer. Their wavelengths are listed in Table 5 along with the current 'best-fit' stick spectral wavelengths (see Table 3). Agreement is reasonably good in the long wavelength half of the Q_Y region, but not so good at the shorter wavelengths. Indeed, agreement may not even be as good as it appears. Since 6 of the transition energies have not been determined by hole-burning, the positions of the gaps in column 2 of Table 5 are somewhat arbitrary. Thus, the assignment of the 793.6-nm transition as exciton transition #6 in the current numbering is particularly uncertain. The poorer agreement at shorter wavelengths of calculated transition wavelengths with these experimental results is most likely one more indication that the choices of BChl Q_Y site energies in the calculations are not optimal, especially for BChls 1–5. On the other hand, the agreement for the two longest-

Table 5. Comparison with laser hole-burning results[a]

Exciton transition #	Wavelength (nm)		Absorption width (cm^{-1})	
	Hole burning[b]	This work	Hole burning[b]	This work
1		779.7		170
2, 3		780.4		170
4, 5		789.4		170
6	793.6	789.8	80	170
7, 8		797.4		170
9	801.3	799.6	80	170
10	804.8	803.8	80	170
11, 12	807.8	805.5	80	80
13	813.0	813.0	80	85
14, 15		814.3		85
16		814.7		85
17, 18	816.3	815.3	80	85
19	824.4	824.1	70	80
20, 21	827.1	826.4	70	80

[a] Johnson and Small (1991).
[b] See text for details of these assignments.

wavelength transitions is almost certainly no accident. It is clear from the calculations that the splitting of these two transitions arises almost entirely from the intersubunit (C-3 symmetric) interactions of the BChls 7. Johnson and Small (1991) reached this same conclusion on the basis, in part, of polarized hole-burning spectroscopy.

Absorption line widths of the individual exciton transitions deduced by Johnson and Small (1991) in part from their experimental hole-burning results are also listed in Table 5. Again, these are seen to agree reasonably well with the widths used in the present calculations, at least for the longer wavelength transitions. The disagreement at the shorter wavelengths may also be attributable mainly to suboptimal site-wavelength choices. However, other factors may be involved as well. One of these factors is line shape. Johnson and Small (1991) argue that while an inhomogeneously broadened line may be well approximated by a symmetric Gaussian, a homogeneously broadened line should be represented by a Lorentzian. Of the 8 transitions that they characterize (Table 5), the 6 at shortest wavelength are deduced to be mainly homogeneously broadened, and the two at longest wavelength to be almost entirely inhomogeneously broadened. Thus, they argue, all but the latter two transitions should be represented by Lorentzians. A theoretical absorption spectrum calculated from Lorentzian components is shown in Fig. 6. (The model with common site wavelengths is chosen for this calculation because it lacks the 825-nm region transitions, and the uniform site wavelengths appear to better represent the shorter wavelength region.) Aside from the obviously too small overall transition strength (see discussion of this parameter above), the effects of which are accentuated by the very broad tails of the Lorentzians, it may be seen by comparing Figs. 3 and 6 that the use of Lorentzians for the shorter-wavelength components probably does improve the fit to the experimental absorption spectrum. However, because of the current uncertainties in the input parameters of the calculation, one must exercise caution in reaching this conclusion.

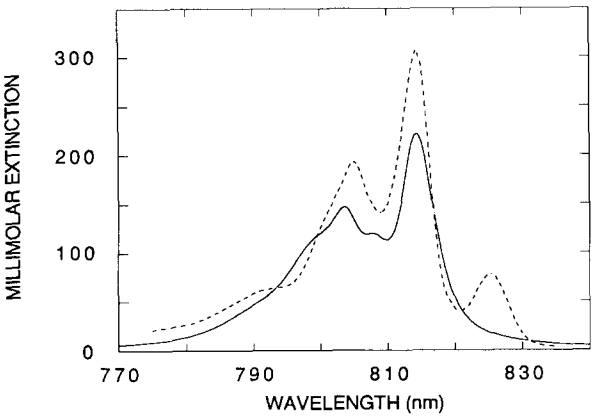

Fig. 6. Theoretical absorption spectrum (solid curve) for a trimer with the same common site wavelength as in Fig. 3, but synthesized from symmetric Lorentzians rather than Gaussians. The Lorentzians have full-widths at half maximum of 170 cm^{-1} for exciton transitions 1–10, 80 cm^{-1} for transitions 11–15, and 70 cm^{-1} for transitions 16–21. The dashed curve is the experimental spectrum (see Fig. 2).

3.6. Some remaining problems

The most critical problem is more precise determination of the adjustable parameters. In the near term this is most likely to be accomplished by machine search with the aid of a suitably efficient algorithm. However, given the complexity of the problem, the selection and successful execution of such an algorithm is not likely to be trivial. There are, in addition, issues related to spectral line shape. It is by no means certain that a simple model, such as is used here, in which each exciton transition is represented as a single symmetric Gaussian or Lorentzian, will suffice.

One would like to see as well various extensions of these spectral calculations. For example, it is in principle possible to simulate the spectra in the Q_X region. This has been considered less interesting because exciton effects in this region are expected to be much smaller than in the Q_Y, whose overall squared dipole strength is nearly an order of magnitude larger than that of the Q_X. However, despite this and the fact that there is no apparent correlation of Q_X and Q_Y site wavelengths, good experimental spectra of the Q_X region exist (Philipson and Sauer 1972) and remain to be interpreted. Another obvious extension is to the calculation of linear dichroism spectra. Here, there is an additional difficulty, i.e., determining the relation of the macroscopic alignment axis to the geometry of the protein

trimer. Unless the trimer's C-3 axis is parallel to the alignment axis, which is unlikely in the case of electric-field alignment (Whitten et al. 1978b), it may be necessary to consider alignment of aggregates of trimers, and to develop geometric models of those aggregates (Matthews et al. 1977). Again, good experimental spectra exist (Whitten et al. 1978b, Swarthoff et al. 1980).

There is also a question of the ultimate precision with which one can expect to simulate the experimental optical spectra. The absorption (Whitten et al. 1980), and especially the CD (Philipson and Sauer 1972, Olson et al. 1976) spectra are noticeably dependent on the mixture of cryosolvents used for the measurement. This means that such solvents at least slightly perturb the protein structure or modify the site-wavelength-determining interactions. This limitation might be overcome should it become possible to obtain high-resolution spectra of crystalline samples. However, in that case, spectral simulations may have to take into account the intertrimer interactions in the crystal, some of which may be comparable in magnitude to the intratrimer interactions that have been demonstrated here to have spectral significance.

4. Conclusions

It now appears likely that the absorption and CD spectra of the BChl *a* protein from *P. aestuarii* will be understood in terms of the unaggregated trimer. This is a result of avoiding the non-standard assumption regarding Q_Y transition moment directions made by Pearlstein and Hemenger (1978), of introducing a reasonable set of BChl site wavelengths, and of including all 21 BChls of the trimer (rather than just the 7 BChls of one subunit) in the exciton calculations. Improvements to the current fit by further refinement of site wavelengths and use of more realistic spectral line shape fitting methods are to be expected. It is already clear that, whatever the final assignments of site wavelengths, that of BChl 7 in each subunit must be the longest one. At low temperature, at least, the lowest energy exciton state, to which this molecule is the largest contributor, is expected to serve as a singlet excitation energy trap for the antenna complex.

Rationalizing the individual site wavelengths in terms of the properties of each BChl molecule and its interactions with the protein will not be easy, as demonstrated by the molecular orbital calculations of Gudowska-Nowak et al. (1990).

Further substantiation of this trimer exciton-interaction model must come from comparison of calculated spectra with experimental optical spectra of other sorts, for example, linear dichroism.

Acknowledgements

I have benefitted from discussions with my colleagues, J. Fajer, A. Scherz and G. Small.

References

Fenna RE and Matthews BW (1975) Chlorophyll arrangement in a bacteriochlorophyll protein from *Chlorobium limicola*. Nature 258: 573–577

Fenna RE, ten Eyck LF and Matthews BW (1977) Atomic coordinates for the chlorophyll core of a bacteriochlorophyll *a*-protein from green photosynthetic bacteria. Biochem Biophys Res Commun 75: 751–756

Gudowska-Nowak E, Newton MD and Fajer J (1990) Conformational and environmental effects on bacteriochlorophyll optical spectra: Correlations of calculated spectra with structural results. J Phys Chem 94: 5795–5801

Hanson LK (1988) Theoretical calculations of photosynthetic pigments. Photochem Photobiol 47: 903–921

Johnson SG and Small GJ (1991) Excited-state structure and energy-transfer dynamics of the bacteriochlorophyll *a* antenna complex from *Prosthecochloris aestuarii*. J Phys Chem 95: 471–479

Matthews BW, Fenna RE and Remington SJ (1977) An evaluation of electron micrographs of bacteriochlorophyll *a*-protein crystals in terms of the structure determined by x-ray crystallography. J Ultrastruc Res 58: 316–330

Matthews BW, Fenna RE, Bolognesi MC, Schmid MF and Olson JM (1979) Structure of a bacteriochlorophyll *a*-protein from the green photosynthetic bacterium *Prosthecochloris aestuarii*. J Mol Biol 131: 259–285

Meister A (1986) Calculation of exciton interaction between subunits of bacteriochlorophyll-protein from *Prosthecochloris aestuarii*. Studia Biophys 113: 171–176

Olson JM (1966) Chlorophyll-protein complexes part II. Complexes derived from green photosynthetic bacteria. In: Vernon LF and Seely GR (eds) The Chlorophylls, pp 413–425. Academic Press, New York

Olson JM, Ke B and Thompson KH (1976) Exciton interac-

tions among chlorophyll molecules in bacteriochlorophyll *a* proteins and bacteriochlorophyll *a* reaction center complexes from green bacteria. Biochim Biophys Acta 430: 524–537

Pearlstein RM (1982) Chlorophyll singlet excitons. In: Govindjee (ed) Photosynthesis: Energy Conversion by Plants and Bacteria, Vol 1, pp 293–330. Academic Press, New York

Pearlstein RM (1987) Structure and exciton effects in photosynthesis. In: Amesz J (ed) Photosynthesis, pp 299–317. Elsevier Science Publishers BV, Amsterdam

Pearlstein RM (1988) Interpretation of optical spectra of bacteriochlorophyll antenna complexes. In: Scheer H and Schneider S (eds) Photosynthetic Light Harvesting Systems, pp 555–566. Walter de Gruyter and Co, Berlin

Pearlstein RM (1991) Theoretical interpretation of antenna spectra. In: Scheer H (ed) Chlorophylls, pp 1047–1078. CRC Press, Boca Raton

Pearlstein RM and Hemenger RP (1978) Bacteriochlorophyll electronic transition moment directions in bacteriochlorophyll *a*-protein. Proc Natl Acad Sci USA 75: 4920–4924

Pearlstein RM and Zuber H (1985) Exciton states and energy transfer in bacterial membranes: The role of pigment-protein cyclic unit structures. In: Michel-Beyerle ME (ed) Antennas and Reaction Centers of Photosynthetic Bacteria, pp 53–61. Springer-Verlag, Berlin

Philipson KD and Sauer K (1972) Exciton interaction in a bacteriochlorophyll-protein from *Chloropseudomonas ethylica*. Absorption and circular dichroism at 77 K. (1972) Biochem 11: 1880–1885

Swarthoff T, de Grooth BG, Meiburg RF, Rijgersberg CP and Amesz J (1980) Orientation of pigments and pigment-protein complexes in the green photosynthetic bacterium *Prosthecochloris aestuarii*. Biochim Biophys Acta 593: 51–59

Tronrud DE, Schmid MF and Matthews BW (1986) Structure and x-ray amino acid sequence of a bacteriochlorophyll *a* protein from *Prosthecochloris aestuarii* refined at 1.9 Å resolution. J Mol Biol 188: 443–454

Weiss C (1972) The pi electron structure and absorption spectra of chlorophylls in solution. J Mol Spectrosc 44: 37–80

Whitten WB, Nairn JA and Pearlstein RM (1978a) Derivative absorption spectroscopy from 5–300 K of bacteriochlorophyll *a*-protein from *Prosthecochloris aestuarii*. Biochim Biophys Acta 503: 251–262

Whitten WB, Pearlstein RM, Phares EF and Geacintov NE (1978b) Linear dichroism of electric field oriented bacteriochlorophyll *a*-protein from green photosynthetic bacteria. Biochim Biophys Acta 503: 491–498

Whitten WB, Olson JM and Pearlstein RM (1980) Sevenfold exciton splitting of the 810-nm band in bacteriochlorophyll *a*-proteins from green photosynthetic bacteria. Biochim Biophys Acta 591: 203–207